

## Automatic organ-level point cloud segmentation of maize shoots by integrating high-throughput data acquisition and deep learning

Yinglun Li<sup>a,c,1</sup>, Weiliang Wen<sup>a,b,1</sup>, Teng Miao<sup>d</sup>, Sheng Wu<sup>a,b</sup>, Zetao Yu<sup>b</sup>, Xiaodong Wang<sup>b</sup>, Xinyu Guo<sup>a,b,\*</sup>, Chunjiang Zhao<sup>a,b,c,\*</sup>

<sup>a</sup> Information Technology Research Center, Beijing Academy of Agriculture and Forestry Sciences, Beijing 100097, China

<sup>b</sup> Beijing Key Lab of Digital Plant, National Engineering Research Center for Information Technology in Agriculture, Beijing 100097, China

<sup>c</sup> College of Resources and Environment, Jilin Agricultural University, Changchun 130118, China

<sup>d</sup> College of Information and Electrical Engineering, Shenyang Agricultural University, Shenyang 110161, China



### ARTICLE INFO

#### Keywords:

High throughput  
Point cloud segmentation  
Deep learning  
phenotype  
Maize  
Pipeline

### ABSTRACT

Point cloud segmentation is essential for studying the 3D spatial characteristics of plants. Notably, the segmentation accuracy greatly impacts subsequent 3D plant phenotypes extraction and 3D plant reconstruction. Automated segmentation approaches for plant point clouds are a bottleneck in achieving big data processing of 3D plant phenotypes. Using maize as a representative crop, this study developed DeepSeg3DMaize, a technique for plant point cloud segmentation that integrates high-throughput data acquisition and deep learning. A high-throughput data acquisition platform for individual plants and an association mapping panel containing 515 inbred lines were used to construct the training dataset. Specifically, the MVS-Pheno platform was used to acquire high-throughput data, and Label3DMaize was used for point cloud data labeling. Based on the dataset, PointNet was introduced to implement stem-leaf and organ instance segmentation, and six phenotypes were extracted. According to the results, the mean precision and F1-Score of stem-leaf segmentation were 0.91 and 0.85, respectively. Meanwhile, the mean precision and F1-Score for organ instance segmentation were 0.94 and 0.93, respectively. The correlations of the six parameters (leaf length, leaf width, leaf inclination, leaf growth height, plant height, and stem height) extracted from the segmentation results with the measured values were 0.90, 0.82, 0.94, 0.95, 0.99, and 0.94, respectively. High-throughput data acquisition, automatic organ segmentation, and phenotypic data extraction form an automatic phenotypic data processing pipeline, which is practical for dealing with large amounts of initial data. Besides, it provides a systematic reference for the automated analysis of 3D phenotypic features at the individual plant level.

### 1. Introduction

Plant phenotypes are determined by plant-environment interactions (Ninomiya et al., 2019; Zhao et al., 2019). The acquisition, identification, and analysis of various plant characteristics and phenotypes are fundamental in both life and agricultural sciences (Dhondt et al., 2013; Zhao, 2019). Traditional plant phenotyping methods are constrained by small scale, having low efficiency, large errors, and weak applicability (Tardieu et al., 2017). Thus, these methods cannot enable systematic studies of plant gene functions (Fasoula et al., 2020) and are a bottleneck limiting plant multi-omics research and molecular design breeding (Chawade et al., 2019). The recent years have evidenced substantial

progress in the application of computer vision-based techniques for high-throughput acquisition of plant phenotypes (Barker et al., 2016). These systems facilitate the efficient and accurate high-throughput acquisition of phenotypes such as plant morphology, structure, color, and texture (Li et al., 2020) and mitigate the challenges associated with traditional plant phenotyping techniques (Ghanem et al., 2015).

At present, the rapid development of sensing technology and the improvement of computational performance have enabled rapid data acquisition and phenotype extraction on a 3D scale (Jin et al., 2021; Lin, 2015; Qiu et al., 2018). For instance, LiDAR (Panjvani et al., 2019), depth cameras (Hu et al., 2018; Li et al., 2017), and multi-view imaging techniques (Wu et al., 2020; Wu et al., 2019) are used for 3D plant data

\* Corresponding authors at: Information Technology Research Center, Beijing Academy of Agriculture and Forestry Sciences, Beijing 100097, China.

E-mail addresses: [guoxy73@163.com](mailto:guoxy73@163.com) (X. Guo), [zhaojc@nercita.org.cn](mailto:zhaojc@nercita.org.cn) (C. Zhao).

<sup>1</sup> Co-first authors.

acquisition (Wang et al., 2018). These tools can extract various phenotypic parameters, such as leaf area, leaf inclination, stem height, and plant volume (Guo et al., 2018; Madec et al., 2017; Qiu et al., 2019). One of the bottlenecks in plant 3D phenotype studies at the organ or individual plant level is how to segment a 3D point cloud data of a shoot to multi-organs (Paulus, 2019; Paulus et al., 2013; Kuhlmann et al., 2014). The currently available plant 3D data segmentation techniques mainly focus on individual (Das Choudhury, et al., 2020) and population scales (Walter et al., 2019), such as geometry-based (Wu et al., 2013), threshold-based (Yang et al., 2013), and machine learning-based approaches (Ziamtsov et al., 2020). Among these, the geometry-based and threshold-based methods require heavy manual interactions. The segmentation results depend on the setting of empirical parameters, which cannot meet big-data processing requirements in plant phenotyping studies (Jin et al., 2019). In general, the current plant 3D data processing techniques are time-consuming and require many manual interactions, resulting in a large amount of raw data accumulation. Besides, the approaches constraint the high-throughput resolution of phenotypic indicators of interest to agronomists. Subsequently, the actual value of data cannot be explored (Pieruschka and Schurr, 2019). It is, therefore, urgent to design and develop new methodologies to improve the throughput and automation level of plant-to-organ 3D data segmentation of plants (Sarkar et al., 2016; Ziamtsov and Navlakha, 2019). Machine learning methods can be algorithmically designed to extract features from large data amounts automatically; in particular (Mochida et al., 2019), deep learning has provided new perspectives for solving these problems (Jiang et al., 2019; Ubbens and Stavness, 2018).

Applying deep learning techniques to plant 3D data processing and phenotype extraction is challenging and promising (Ziamtsov and Navlakha, 2019). Notably, segmentation of 3D point clouds using deep learning is an emerging research field (Li et al., 2020; Bernotas et al., 2019; Liu et al., 2019). Researchers in this field use annotated voxel (Jin et al., 2020) or multi-view grayscale images (Shi et al., 2019) to train deep neural network models, thus achieve organ instance segmentation from individual plants to organs of 3D point cloud data. Both methods aim to obtain segmented plant point clouds but do not use the point cloud data to train the model. Deep learning-based plant segmentation utilizing point clouds as inputs has been reported by Turgut et al. (2020). They segmented rosebush plants into blocks, and the point cloud in each block was segmented by the neural network. The predictions from the blocks were then integrated to obtain a full segmentation. Although similar to voxels, separating a plant into blocks enable point-based deep learning architectures to accept fixed-size data as input.

Training deep learning models using point cloud data is still challenging (Jin et al., 2021). Firstly, point cloud data is disordered and has rotational invariance (Charles et al., 2017a,b; Yin et al., 2018), which should be addressed during the model training to extract global features (Song et al., 2020; Zhao et al., 2020). Although point clouds contain color information, this feature attribute can hardly be used for model training of predominantly green plants (Kurobe et al., 2020; Lee and Kim, 2019). Secondly, there are few publicly available point cloud datasets for training in the plant domain, and there is no commonly used benchmark data for organ instance segmentation for phenotype extraction. Dutagaci et al. (2020) provided an annotated 3D data set of rosebush plants for training and evaluation of organ segmentation methods. However, only 11 plants were included in the training dataset, and preprocessing operations are required for deep-learning segmentation tasks. Besides, the dataset is inapplicable for other plant species. Compared to 2D images, where data enhancement is often used to build datasets, the spatial features of 3D point clouds suffer rotational invariance. Thus, building 3D datasets in this way is not effective for training deep learning models (Morel et al., 2020; Qi et al., 2018). Using high-quality and diverse raw plant point cloud data is beneficial for training deep learning models to obtain better segmentation results (Perez-Gonzalez et al., 2019; Qin et al., 2020). Therefore, constructing high-quality datasets is also key to 3D point cloud segmentation of

plants by deep learning methods.

Obtaining high-quality 3D point clouds of individual plants in a high-throughput way, as well as efficient annotation of the point clouds, are challenging for deep learning-based plant segmentation tasks. This study proposes DeepSeg3DMaize, an automated maize point cloud processing pipeline, to circumvent the above challenge. MVS-Pheno platform was used to obtain multi-view images, then generate point clouds of individual maize plants in this pipeline. After pre-processing, maize shoots were annotated using Label3DMaize toolkit, then a training dataset was constructed. The PointNet model was then used as the deep learning method to realize automatic point cloud segmentation of maize from individual plant to organs. The organ level phenotyping parameters were eventually extracted from the segmented point clouds. DeepSeg3DMaize achieved a high-throughput and automatic pipeline of maize shoots, and is expected to provide automated and efficient solution for 3D phenotyping of maize shoots.

## 2. Materials and methods

### 2.1. Overview

The DeepSeg3DMaize method mainly consists of five parts (Fig. 1): high-throughput data acquisition of maize shoots, data pre-processing and normalization, data annotation and dataset construction, deep learning-based segmentation of maize shoot point clouds, and phenotypes extraction.

### 2.2. High-throughput data acquisition

To construct a point cloud training dataset covering as many morphological and structural features of maize shoots as possible, a maize association mapping panel containing 515 inbred lines was selected (Yang et al., 2010). The field experiment was conducted in 2019 at the Beijing Academy of Agriculture and Forestry ( $39^{\circ}56'N$ ,  $116^{\circ}16'E$ ). The sowing date was 17 May 2019, and the rows were planted 60 cm apart. The maize plants in each row were 27.8 cm apart, with each cultivar planted individually in an area of two sqm. Maize point cloud data were collected at V3 (three leaf stage), V6 (six leaf stage), V9 (nine leaf stage), and V12 (twelve leaf stage) growth stages (Abendroth, 2011), respectively. To ensure the quality of the sample data, 1–3 plants of each cultivar were obtained at each growth stage of interest. For cultivars with low emergence rates, more than three shoots were planted to ensure the required sample numbers in subsequent experiments.

High-throughput data acquisition was performed using MVS-Pheno (Wu et al., 2020) (Fig. 1a), a semi-automated multi-view image acquisition platform for individual plants. Target plant shoots grown in the field were transplanted into pots, then about nine shoots were transported using a tricycle to the nearby laboratory where the MVS-Pheno was deployed. Two persons were needed during the above process. The time-cost from field to the MVS-Pheno platform depends on the distance between the two positions, and was less than 10 min in this study. Once a shoot has been manually placed on the platform, cameras can be driven by a control command unit to rotate  $360^{\circ}$  around the shoot to capture images from different angles of view. In this study, 2–4 cameras were used (depending on the size of the plant at each growth stage), each taking around 40 images in two minutes. The Multi-view 3D reconstruction technique was applied to achieve the 3D reconstruction of the point cloud of each shoot. The platform's efficiency in acquiring individual maize plants is 1–2 min per shoot. Thus, it would theoretically take no more than 51.5 h to acquire the point clouds for all the 515 cultivars during a specific growth period. For growth stages during which maize grows faster, multiple devices are used to shorten the data acquisition cycle. Besides, the maize plants were transplanted in the field into pots then moved greenhouse, where the data was obtained in a stable, wind-free environment. To prevent plant morphological changes after transplanting, the plants were properly watered, and data were

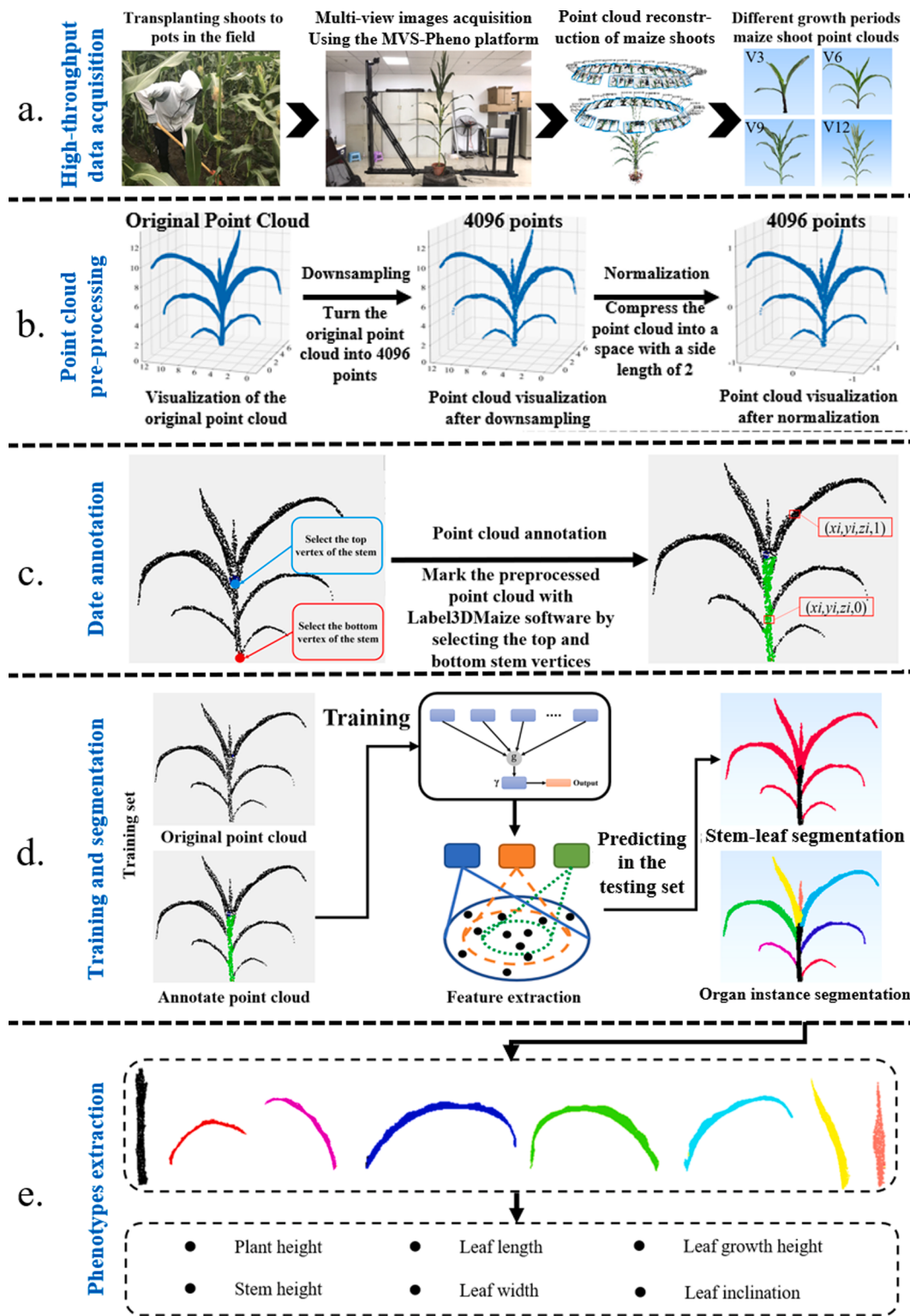


**Fig. 1.** Methodology flow chart. (a) High-throughput data acquisition of maize shoots using the MVS-Pheno phenotyping platform. (b) Point cloud pre-processing, including point cloud down-sampling and normalization. (c) Data annotation using the Label3DMaize software and dataset construction. (d) Training with PointNet for stem-leaf and organ instance segmentation. (e) Extraction of phenotypes using organ instance segmentation results.

acquired within two hours. Also, the phenotypic parameters of 25 maize shoots (including ten cultivars from inbred lines and 15 cultivars from hybrids) were measured to evaluate the segmentation performance of DeepSeg3DMaize on inbred lines and hybrid cultivars, and to validate the resolved parameters. These features included plant height, stem height, leaf growth height, leaf inclination, leaf length, and leaf width.

### 2.3. Dataset construction

#### 2.3.1. Point cloud Pre-processing

The point clouds reconstructed using the MVS-Pheno platform are dense, containing around 5 to 13 million points per plant. The reconstructed scene was a dense point cloud with a maize shoot, a pot, and

ground. The point cloud of target maize shoot should be segmented, then simplified to less than 100,000 points. Then, a uniform down-sampling method was used to control the number of points in each plant point cloud to a range of 4096, improving the efficiency of subsequent model training. Each point cloud was then transformed to a cube with sides of length 2 cm and centered at the origin for normalization. The down-sampling and normalization operations change the actual size of the data; however, it is possible to effectively reduce the amount of input to the training data while ensuring detailed plant morphological features. The transformation matrix of normalization was recorded. In later calculations, the plants can be de-normalized to their true size by inversion and up-sampling using the normalization matrix, thus does not affect the accuracy of subsequent phenotypic parameter extraction. An illustration of point cloud pre-processing is shown in Fig. 1(b).

### 2.3.2. Point cloud annotation

At present, no commonly used 3D point cloud annotation software can segment the point clouds. Most point cloud annotations were conducted using open-source software such as CloudCompare and MeshLab (Ghahremani et al., 2021). However, these tools often require a great deal of interaction to achieve accurate point cloud segmentation annotations. Furthermore, none of the existing methods can achieve accurate annotation of point cloud data with an accuracy comparable to image data.

In this study, Label3DMAize (Miao et al., 2021) was used to annotate the training data for stem-leaf segmentation. Label3DMAize is a toolkit developed by our research group for maize plants. The software selects the top and bottom stem points in the maize point cloud and adjusts the corresponding radius both via manual interaction. The median region growing method is then applied to achieve automatic segmentation and labelling of the maize stem and leaves. Suppose the connection area between the stem and leaves is not accurately annotated. In that case, the toolkit provides a fine segmentation function that allows correction of the misclassified points through simple manual interaction. Tests have shown that automatic annotation results obtained by the toolkit are satisfactory for model training. Stem points are labelled by 0, while leaf points are labelled by 1. The labelling of each shoot using the Label3DMAize software only takes about 30 s. Besides selecting the stem endpoints and adjusting the radius parameters, all other procedures are automated and are performed with good efficiency. The data annotation is illustrated in Fig. 1(c), while the final annotated data is encapsulated with the original point cloud into the HDF5 format and sent to the model for training. Since the fine segmentation function in Label3DMAize can improve the segmentation accuracy of point clouds, the instance segmentation accuracy was evaluated using the results obtained using fine segmentation as true values.

### 2.3.3. Dataset composition

Data screening, which involves evaluating the software morphometrics and the point cloud quality of all the shoots, must be performed to build a high-quality dataset. The dataset constructed for this study consisted of 1600 plant samples, with 1500 in the training set and 100 in the testing set. The training set contained 500 V3 and 1000 V6 point clouds. As maize shoots are mainly composed of leaves and stem before tassel emergence, some point cloud data from V9 and V12 were thus added to the testing set to validate the segmentation performance of the DeepSeg3DMAize. The same annotation method was applied to annotate the samples in the test set, with each plant point cloud divided into stem and leaf instances. All plant point clouds were down-sampled and normalized. Significantly, all 1600 point clouds were obtained from actual samples but were not expanded in any way. As the point cloud data form differs significantly from the image form, the commonly used image dataset expansion approaches through data augmentation is not applicable to point cloud datasets. Since point cloud transformation of a whole plant does not improve deep learning-based model, useless data augmentation worsens the dataset quality. In this study, the high-

throughput platform was used to obtain enough samples and avoid data expansion to degrade the dataset quality and affect the model performance. The specific data set composition is shown in Table 1.

## 2.4. Segmentation network

### 2.4.1. Training by PointNet

PointNet (Charles et al., 2017a,b) is the first deep neural network that can directly process unordered point cloud data. The network is mainly used to classify and segment point clouds, and its model framework is also divided into two: the classification model and the segmentation model. Notably, the PointNet segmentation model is an extension of its classification model. While classification aims for overall abstraction of a point cloud and mapping it to a category domain, the essence of segmentation is to abstract a point cloud as a whole and then map the local features to different semantic intervals. Thus, the segmentation problem can be solved by converting it into a classification problem. The specific PointNet model framework used for segmentation in this study is shown in Fig. 2. The main highlights of the model structure are the T-Net and MLP operations.

The network input data include point clouds of plants containing N points and  $N \times 3$  coordinate information. The original data is passed through the first T-Net transformation matrix to achieve data alignment and ensure model invariance for specific spatial transformations. Aligned data, which is extracted point-by-point, is characterized by a multi-layer perceptron with shared parameters. The 64-dimensional features of each point were extracted, and the second spatial feature transformation matrix of the network was predicted by T-Net, which was adjusted to a transformation matrix of  $64 \times 64$  sizes for feature alignment at a later stage. The global feature vector of each point cloud was extracted via a max pooling layer. Finally, global features were passed through the MLP multi-layer perceptron (512, 256, k) to produce k classifications, where k represents the classification category (i.e., the number of categories defined by the label). Each category corresponded to the classification score of the point cloud. During point cloud segmentation by PointNet, the global (the output of the MLP) and local features (the result of applying the second T-Net network transformation) of the model output were cascaded according to the output of each layer based on the network structure described above. For stem-leaf semantic segmentation, the parameter k was set to 2 in the model output and could divide the overall point cloud into two categories: stem and leaf. In contrast, organ instance segmentation must be processed based on the stem-leaf segmentation results. For organ instance segmentation, the model incorporates a local feature extraction operation that extracts local features at different scales to obtain deep features through the multi-layer network structure described above (Qi et al., 2017). The deep features are fused with the cascade output of each network layer, and then the fused features are clustered by the Mean-shift algorithm (Yizong, 1995) to obtain the effect of instance segmentation of organs.

### 2.4.2. Feature extraction

Deep learning methods have powerful feature extraction capabilities; thus, they can learn useful features in huge amounts of data independently. In 2D convolutional neural networks, the relevant features can be extracted efficiently using traditional convolutional methods.

**Table 1**

Sample composition of the training and testing sets.

Stage	Number of training	Number of testing sets
V3	500	30
V6	1000	50
V9	–	10
V12	–	10
Overall	1500	100

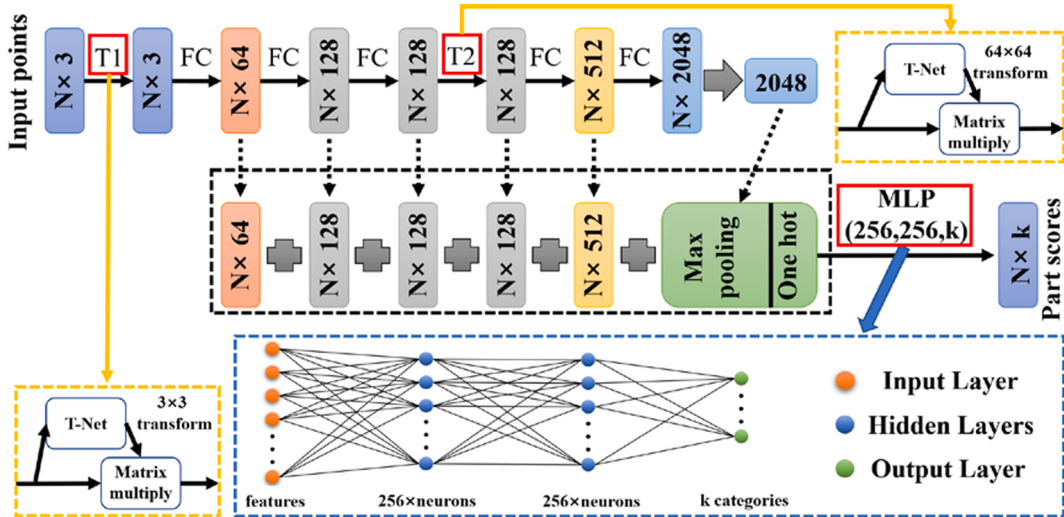


**Fig. 2.** Structure of the PointNet model for segmentation. In this case, T-Net is a spatially transformed matrix prediction network for estimating the prediction matrix. MLP stands for Multi-Layer Perceptron, and the number in brackets is the layer size. The network takes the point cloud as input, applies the input and feature transformations, and then aggregates the point features through the max pooling. In the figure above, T1 and T2 indicate different T-Net treatments, corresponding to the two yellow dashed boxes indicated by the arrows. The MLP structure is indicated by the blue dashed box shown by the downward arrow.

However, the disorderly nature of the point cloud in 3D networks constrains feature extraction by conventional convolution operations. To extract the corresponding features in 3D point cloud data, PointNet has designed a set of feature functions.

Further, to solve point disorder in point clouds, PointNet introduces a simple symmetric function that integrates the information of each point to enhance order in the point cloud (Guibas et al., 2017). This symmetry function takes a vector (the 3D coordinates of a point) as input and outputs a new vector that is invariant with respect to the input order. By applying the symmetry function to the feature extraction result, a general function defined on the set of points is thus estimated. The max pooling layer is used as the main symmetry function to aggregate information from all points, thus solving the constraint of unordered point clouds. The specific feature extraction function is as follows:

$$f(p_1, p_2, p_3, \dots, p_n) \approx \gamma^* g(h(p_1), h(p_2), h(p_3), \dots, h(p_n)) \quad (1)$$

where  $p$  represents a point in the point cloud and  $f(x_1, x_2, x_3, \dots, x_n)$  indicates that the unordered point cloud input is a continuous set function and can map any set of points to a vector;  $h(p_n)$  represents the feature extraction layer and is composed of the single variable function and the maximum merge function;  $g(p)$  is a symmetric function,  $\gamma$  represents higher dimensional feature extraction,  $g(p)$  and  $\gamma$  form the MLP network of the module (Fig. 3). The final output features are selected for

each dimension as the corresponding maximum eigenvalue or sum of eigenvalues in the point cloud; this resolves the disorder by  $g(p)$ .  $g(p)$  can be used for either maxpooling or sumpooling; maxpooling was used in this study. The specific feature extraction is shown in Fig. 3. This function ensures that the value of the continuous setup function in Equation (1) is constant regardless of the point cloud input order.

The output of the above step is a vector that characterizes the global features. For classification problems, an SVM or MLP classifier can be trained directly to determine the class based on the given global feature vector. However, for point segmentation problems, it is necessary to evaluate both global and local features. The global features are cascaded behind the local features of each point, and new point-local features are learned on top of this, where each point contains both local and global features.

#### 2.4.3. Loss function

The Softmax cross-entropy function was used as a loss function during training and defined as follows:

$$\text{Loss} = \sum_{n=1}^N (-y_n \times \log(\hat{y}_n)) + L_{\text{reg}} \quad (2)$$

where  $n$  is the total number of points in the input point cloud;  $y_n$  is the ground truth of the multi-level classification corresponding to this point cloud;  $\hat{y}_n$  is the probability of the output of each point cloud category using the Softmax function;  $L_{\text{reg}}$  denotes the matrix used to constrain the characteristic transformation matrix. The specific formulae for  $\hat{y}_n$  and  $L_{\text{reg}}$  are:

$$\hat{y}_n = \frac{e^{J_n}}{\sum_i e^{J_i}} \quad (3)$$

$$L_{\text{reg}} = \|I - AA^T\|^2 \quad (4)$$

where  $J_n$  denotes the feature extraction results for the  $n^{\text{th}}$  point of the Softmax function input;  $A$  is the feature alignment matrix predicted by the spatial transformation matrix prediction network (T-Net);  $I$  is the unit matrix. According to equation (3) for the known  $n^{\text{th}}$  input point, the value of  $J_n$  was calculated by the following equation:

$$J_n = w \times q_n \quad (5)$$

where  $w$  is the weight of the network as a whole, and  $q_n$  is the input parameter for the  $n^{\text{th}}$  point in the point cloud.

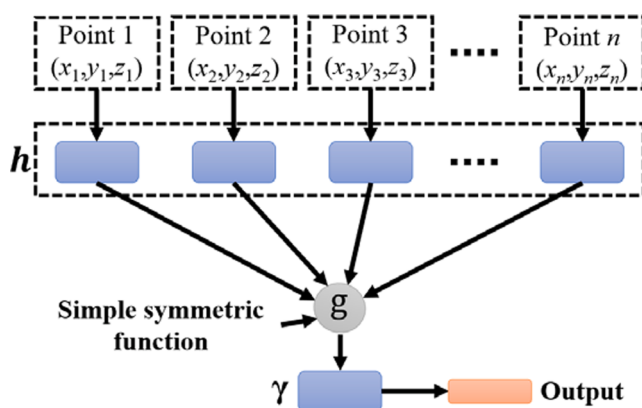


**Fig. 3.** Schematic presentation of feature extraction.

## 2.5. Network training

PointNet was trained using the Tensorflow framework. The training samples from the training set were fed into the network, and the batch size was set to 1. During training, the initial learning rate was set to 0.0001. The ADAM optimizer and stochastic gradient descent (SGD) were used to optimize the learning rate over time. In the model, a weight decay of 0.0001 and a momentum of 0.9 were used. The weights ( $w$ ) of each layer of the deep convolutional neural network were updated by the SGD algorithm. The first layer was the container that received the weighted input, which was then transformed using a set of non-linear functions, then these values were passed on as output to the next layer. If the training loss function is less than a certain loss threshold (i.e., convergence), training is stopped, and the weights of the fixed network layers no longer change, resulting in a deep convolutional neural network after training.

## 2.6. Evaluation indicators

Segmentation accuracy analysis for each predicted point was carried out using the Ground Truth annotation. If a point in the maize plant point cloud is labelled and split into the same class, it is judged as a true positive (TP); if a point is mis-segmented, it is judged as a false negative (FN); if a point label does not exist but is split from an instance or point, then it is judged as a false positive (FP). Generally, high accuracy is expected with higher TP, lower FN, and lower FP (Goutte and Gaussier, 2005). The above metrics can be applied to determine the precision (P), recall (R), and F1-score (F) of point classification on stems and leaves to assess segmentation accuracy. The specific formula was as follows:

$$P = \frac{TP}{TP + FP} \quad (6)$$

$$R = \frac{TP}{TP + FN} \quad (7)$$

$$F = \frac{2PR}{P + R} \quad (8)$$

We also compared the results of manual measurements and that from phenotypic parameters extracted in the PointNet model segmentation. The correlation coefficient ( $R^2$ ) and root mean square error (RMSE) were calculated to compare the results, which were calculated as follows:

$$R^2 = 1 - \frac{\sum_{l=1}^m (v_l - \bar{v}_l)^2}{\sum_{l=1}^m (v_l - \bar{v}_l)^2} \quad (9)$$

$$RMSE = \sqrt{\frac{1}{m} \sum_{l=1}^m (v_l - \bar{v}_l)^2} \quad (10)$$

where  $m$  denotes the number of objects to be compared;  $v_l$  indicates the value of the manual measurement result;  $\bar{v}_l$  denotes the values of the phenotypic parameters extracted from the segmentation results according to the PointNet model;  $\bar{v}_l$  indicates the mean of manual measurement results.

## 2.7. Phenotypic parameter extraction

The DeepSeg3DMaize method was used to segment maize shoots into organ instances. Subsequently, six phenotypic parameters were extracted, including plant height, stem height, leaf growth height, leaf length, leaf width, and leaf inclination. Among the six, plant height, stem height, and leaf growth height were grouped as height categories. Plant height was calculated as the maximum z-value minus the minimum z-value in the point cloud for the entire plant; stem height was calculated by subtracting the minimum z-value from the maximum z-value in the stem point cloud; the leaf growth height was expressed from the maximum z-value of the point on the stem at which that leaf joins the

stem minus the minimum z-value of the stem. The following formulae were used:

$$S_h = z_{max} - z_{min} \quad (11)$$

$$z_{max} = p : (x, y, z) \in S, z \geq z_i, z_{min} = p : (x, y, z) \in S, z \leq z_i \quad (12)$$

where  $x$ ,  $y$ , and  $z$  are the point cloud coordinates while  $z_i$  is the  $z$ -value of the  $i^{th}$  point in the point cloud.

Leaf length and leaf width were calculated using the leaf segmented point clouds. The key feature points in the leaf point cloud were identified from means of internal shape signatures (ISS) (Zhong, 2010), and then the distances between adjacent key feature points were calculated to obtain the leaf length and leaf width by summation. The ISS algorithm calculates the covariance matrix of the key point and its neighbor points after establishing a local coordinate system of a key point in the leaf point cloud. Besides, the relationships between the eigenvalues of the covariance matrix are regarded as feature descriptors of the key points. Meanwhile, the leaf inclination was obtained by calculating the leaf stem angle  $\theta$  as a complementary of the stem-leaf angle. The specific phenotypic parameters extracted are shown schematically in Fig. 4.

## 3. Results

### 3.1. Results for training loss

In this study, the PointNet network was trained with 500 EPOCHs. Each EPOCH contained 1500 batches with a batch size of 1. In the first 100 EPOCHs, the training loss decreased rapidly (Fig. 5), after which the reduction rate in training loss leveled off. The final classification and segmentation losses were 0.002 and 0.055, respectively. The total time for model training was approximately 54 h, and around 10 min for predictions on the testing set. These results were performed on a workstation with 2 Intel Xeon (R) Gold 6148 CPUs, 256 GB RAM, and 2 NVIDIA Quadro P6000 GPUs.

### 3.2. Stem-leaf segmentation

The stem-leaf segmentation results for 100 maize plants in the testing set were evaluated first by visualizing the segmentation point clouds and quantitative indicators. Fig. 6 shows the results of stem-leaf semantic segmentation visualization of a typical maize point cloud at different growth stages in the testing set.

Observation of the stem-leaf segmentation results shows that the output of the prediction by the model correlated to the Ground Truth annotation. The specific segmentation results showed slight differences near the top part, where the leaf clusters articulate with the stem (shown on the right of each subfigure). The quantitative assessment results obtained by evaluating indicators are shown in Table 2. At the point level, the maximum precision was 0.98, while the minimum precision was 0.85 for plants at different growth stages.

### 3.3. Organ instance segmentation results

The organ instance segmentation results for the testing set were also validated by visualizing the segmentation results and quantitative metrics. Fig. 7 shows the organ instance segmentation of the point cloud of representative maize shoots at different growth stages in the test set.

Label3DMaize software was also used to obtain the annotations for the instance segmentation of the leaves in Fig. 7. (Miao et al., 2021). Observation of the DeepSeg3DMaize segmentation results showed that they correlated to the Ground Truth annotation. There were more obvious differences in leaf segmentation in the top leaf cluster of the plant, causing misclassification in the stem portion of the organ instance segmentation. The quantitative assessment results based on the evaluation indicators are shown in Table 2. At the point level, the means of P, R, and F were 0.94, 0.92, and 0.93, respectively.

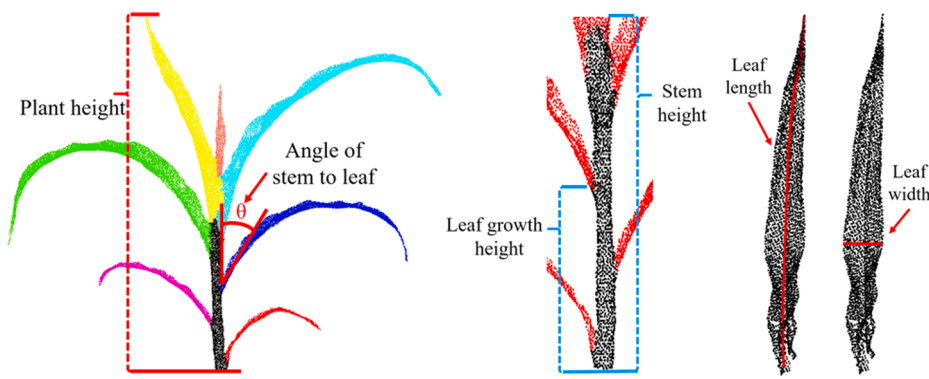


**Fig. 4.** Schematic diagram of phenotypic parameter extraction based on the results of organ instance segmentation.

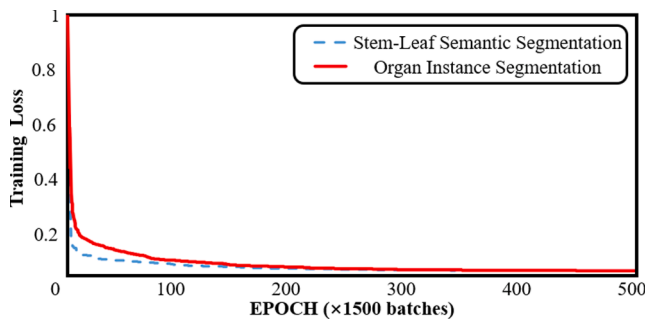


**Fig. 5.** Training losses for stem-leaf semantic segmentation and organ instance segmentation of the model.

#### 3.4. Evaluation of extracted phenotypic parameters

The extracted results were compared with manual measurements to evaluate the accuracy of the extracted phenotypic parameters based on the DeepSeg3DMaize segmentation results. The validation results for each phenotypic parameter are shown in Fig. 8.

In the comparative results for leaf length, leaf width, and leaf inclination (Fig. 8a-c),  $R^2$  and RMSE were 0.90 and 5.58 cm (leaf length), 0.82 and 0.97 cm (leaf width), and 0.94 and 4.18° (leaf inclination), respectively. The correlation between the extracted results for leaf width was low, the correlation for leaf length was medium, while the correlation for leaf inclination was high.

In the comparative results for plant height, stem height, and leaf base height (Fig. 8d-f), the  $R^2$  and RMSE were 0.99 and 0.34 cm (plant height), 0.94 and 10.34 cm (stem height), and 0.95 and 9.15 cm (leaf growth height), respectively. The  $R^2$  of the plant height extraction results by the two methods was close to 1. Meanwhile, the precision of the stem height and leaf growth height extraction results was close to 0.95.

## 4. Discussion

### 4.1. High-throughput data acquisition facilitates High-quality dataset construction

The good performance of the point-based convolutional neural network model on the test sets (including some hybrids) was mainly due to two aspects of the dataset: high quality and diversity.

(1) High-quality data. The original plant point cloud datasets of this study were obtained by the MVS-Pheno platform. The advantage of using this platform to acquire the point cloud data is its high-throughput nature, and the synthesized point cloud data are dense. Besides, the complete plant morphology can still be maintained after down-sampling. Although *in-situ* acquired point clouds are more appropriate for studying the environmental impact on plant phenotypes, using

terrestrial LiDAR is constrained by occlusion, crossover, and overlap of leaves. In addition, de-noising and separating individual plants from the plant population also increases the workload. Using the MVS-Pheno platform to manually select representative and well-grown plants into the plot directly avoids the potential challenges. The quality of the plant point clouds data obtained indoors is better because there is no wind and has stable light environment. High quality data is required to extract phenotypic traits at the cultivar-level. Wind disturbance in the field causes morphological changes in maize, especially at the ends of organs, such as leaf tips and tassels. Besides, field illumination directly affects multi-view images. The reconstructed point cloud using the images acquired in the field always contains a lot of noise and missing points, resulting in a significant error in extracted phenotypic traits, such as plant height, leaf length, and leaf area. However, phenotypes extracted using local or incomplete point clouds, such as leaf angle or azimuth, are less affected.

(2) Data diversity. Data augmentation approaches were always used to increase the amount of the training dataset. Possible data augmentation approaches for point clouds include rotation, translation, scaling, skewing, and stretching. Direct transformation on the whole point cloud could not enhance data diversity since local features do not change during transformation. Jin et al. (2020) used leaf translation and stem stretching for training sample expansion. This point cloud expansion approach aims to develop new local features by shifting the position of leaves and stems. However, points in organ connections were unnatural and had little impact on deep learning. All the point clouds in the training dataset of this study were obtained from different real maize shoots without any data enhancement. The association analysis of the mapping panel material selected for this study showed significant differences among cultivars, and the high coverage of the plant morphological characteristics ensures the complexity and diversity of the training dataset. Therefore, the model performed well in stem-leaf and organ instance segmentation tasks.

In related studies, researchers used terrestrial LiDAR approaches, such as FARO Focus<sup>3D</sup> scanner (Jin et al., 2018), to acquire point cloud data of maize plants. However, this method requires multiple scan stations in different directions (generally more than four stations, and the number of scans depends on the number of scanned plants). For LiDAR, the average scan time is around 5 min, while the MVS-Pheno platform only takes 1–2 min to acquire the raw data of a maize shoot. Specifically, MVS-Pheno is not necessary in the whole processing pipeline and can be replaced by any multi-view image acquisition methods and equipment, including manual image acquisition. A shoot point cloud reconstruction using 120 images takes 20 min in post-processing, and a reconstruction using 60 input images takes only 5 min. Point cloud scaling and shoot segmentation from reconstructed scene are achieved automatically using the data processing system in MVS-Pheno.

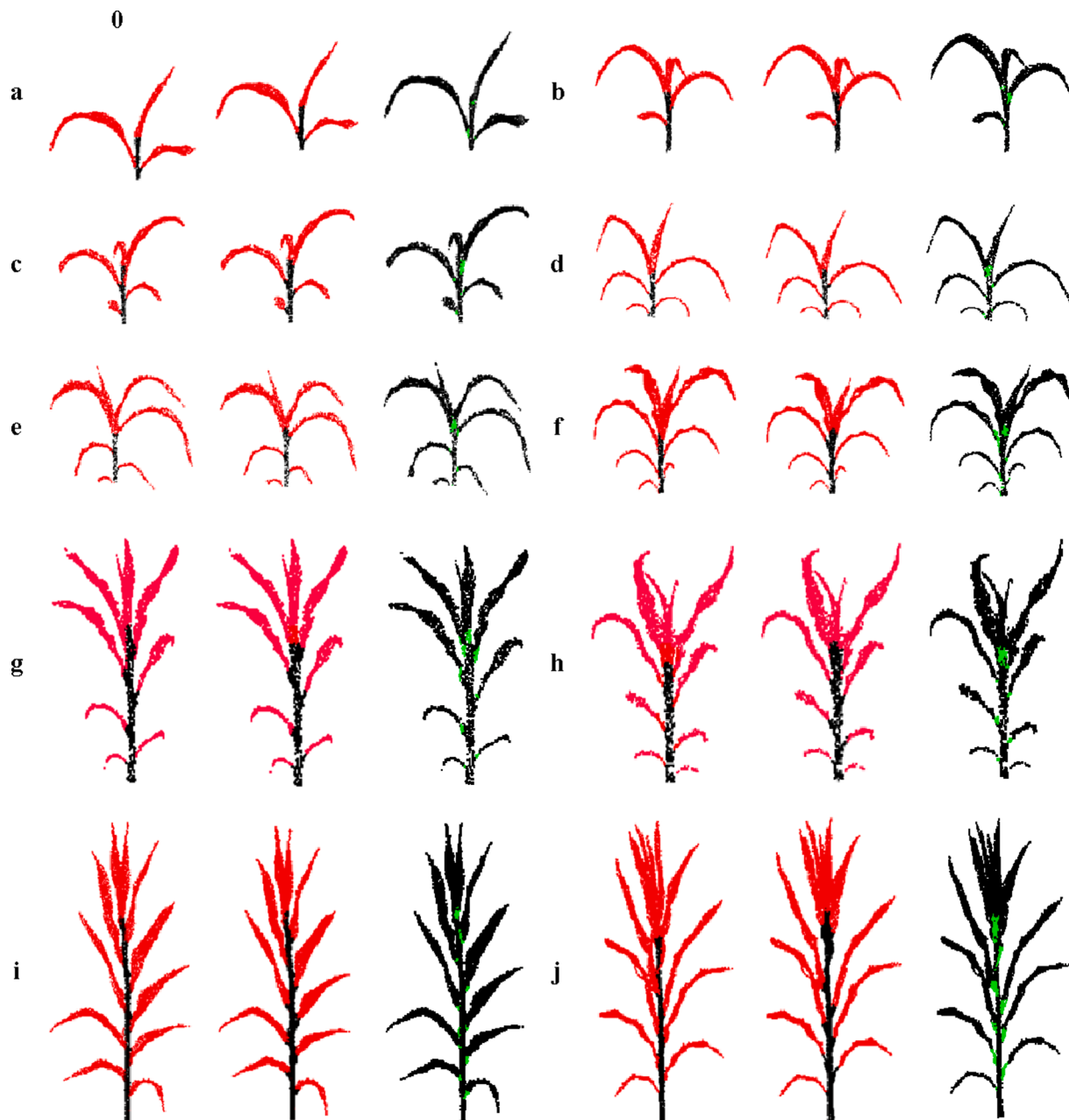


**Fig. 6.** Visualization of stem-leaf semantic segmentation results using DeepSeg3DMAize data for representative data from different growth stages in the testing set. The fine segmentation results using the Label3Dmaize software are shown on the left of each subfigure, while the segmentation results using DeepSeg3DMAize are shown on the middle. The points with different segmentation results in each plant were colored green and shown on the right of each subfigure. The dots on the stems are indicated in black and those on the leaves in red. The number of leaves on plants (a)-(j) increased from 3 to 12.

**Table 2**

Accuracy evaluation of DeepSeg3DMAize for stem-leaf and organ instance segmentation of the testing set.

Evaluation indicators	Stem-leaf segmentation			Organ instance segmentation		
	P	R	F	P	R	F
Max	0.98	1.00	0.99	0.99	0.99	0.99
Min	0.85	0.58	0.69	0.71	0.69	0.70
Mean	0.91	0.79	0.85	0.94	0.92	0.93

#### 4.2. Segmentation accuracy

DeepSeg3DMAize achieved a more accurate point cloud segmentation for maize plants with different leaf numbers at key growth stages

within V<sub>3</sub>-V<sub>12</sub>. However, the DeepSeg3DMAize segmentation results differed slightly from the manually labeled point clouds, mainly at the top leaf clusters and stem-leaf junctions. Regarding the segmentation results of the test set, the accuracy and F score of stem-leaf and organ instance segmentation were 0.85 and 0.93, respectively. Overall, these results suggest that DeepSeg3DMAize is robust for various maize shoots with different plant heights, growth periods, and leaf numbers.

However, DeepSeg3DMAize still has some shortcomings, especially in segmenting the top leaf clusters. Also, this is currently a common problem of point cloud segmentation of maize shoots. Sruti Das Choudhury et al. (Das Choudhury et al., 2020) segmented these organs as a separate whole and named them the TLC (Top leaf cluster). Besides, the newly developed leaves at the shoot apices are tightly packed or wrapped around each other before the tassel emergence. Because it is

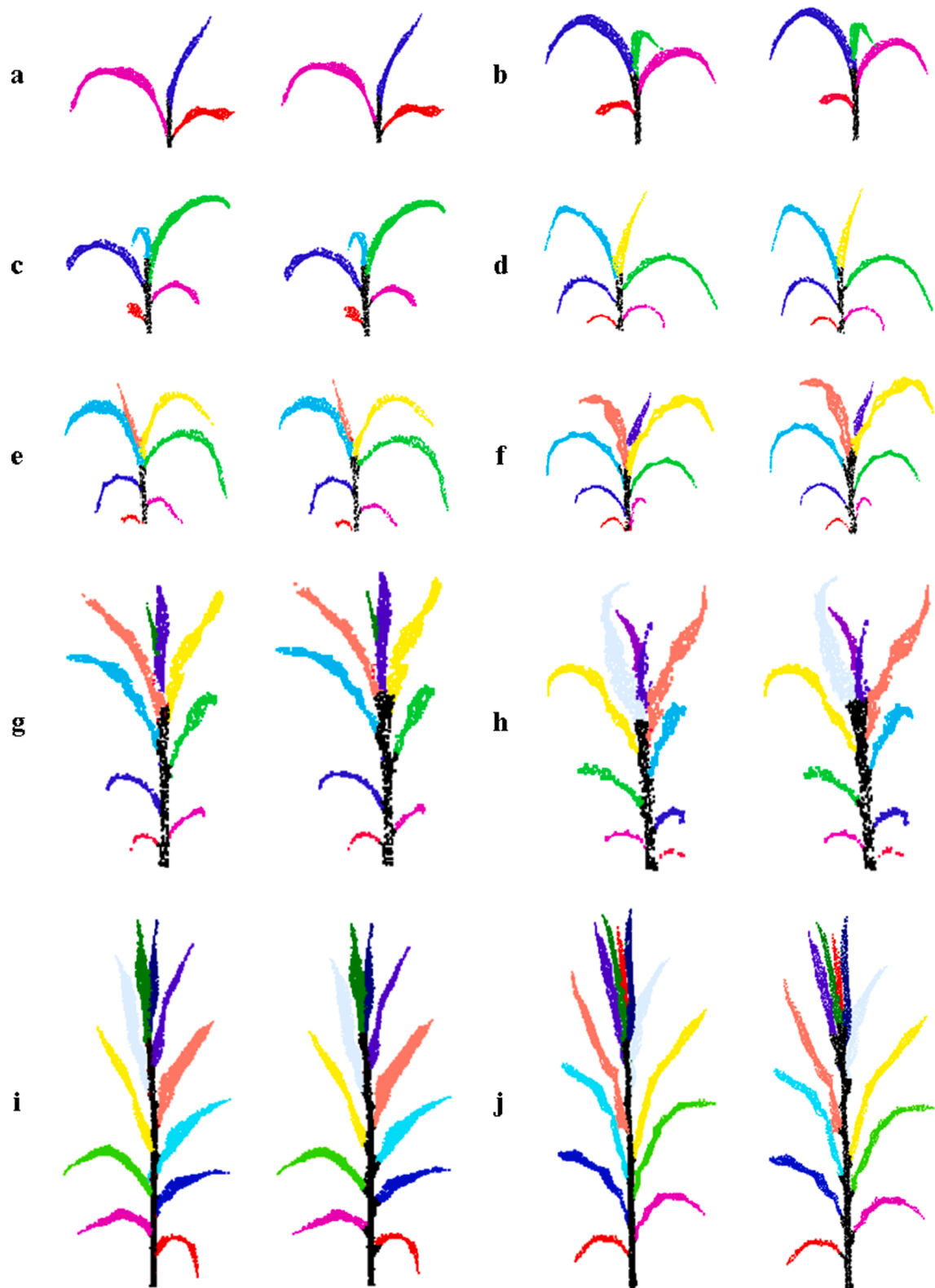


**Fig. 7.** Visualization of organ instance segmentation results using the DeepSeg3DMaize representative data from different growth stages in the testing set. The fine segmentation results using the Label3DMaize software are shown on the left of each subfigure, while the segmentation results using DeepSeg3DMaize are shown on the right. The point clouds on the stems are shown in black, while the leaf point clouds are broken down into each instance and shown in different colors. The leaf numbers on the plants in (a)-(j) of the graph increased from 3 to 12.

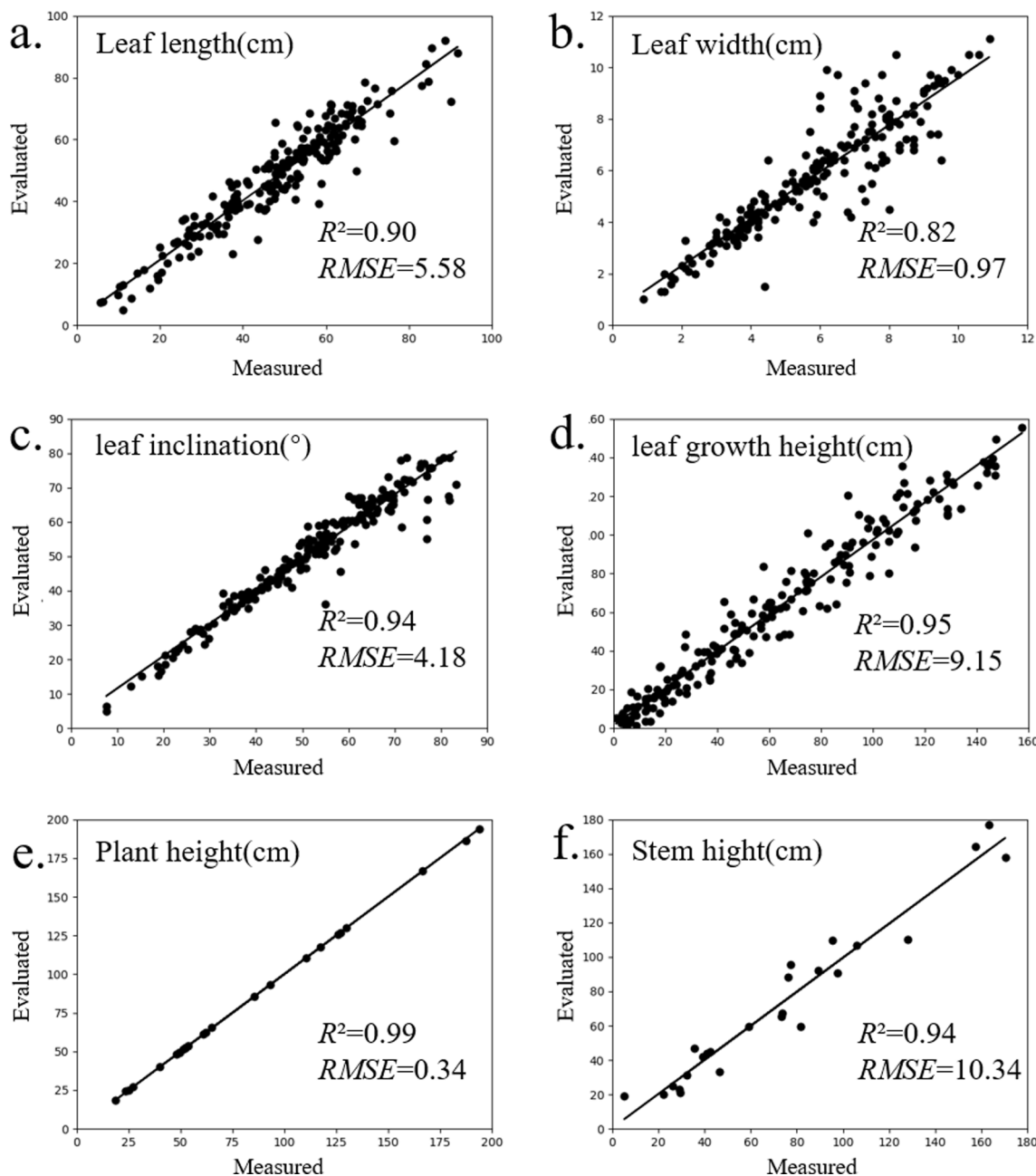


**Fig. 8.** Comparison of phenotypic parameters extracted based on DeepSeg3DMaize point cloud segmentation and measured values. (a) leaf length, (b) leaf width, (c) leaf inclination, (d) leaf growth height, (e) plant height, (f) stem height.

hard to determine the topmost point of the maize stem, even via manual observation, a certain degree of error in the model segmentation of the top leaf clusters and determination of the stem height should be acceptable. In addition, we found that training the model with independent samples is beneficial to improve the accuracy. Thus, the batch size was set to 1 in this study. However, small batch size often leads to overfitting or underfitting. Suitable optimizers and SGD algorithms are helpful for alleviating overfitting or underfitting problems.

Correlation analysis of the extracted phenotypes revealed that the correlation of leaf width parameters was lower ( $R^2 = 0.82$ ) than the other five parameters. This finding could be due to more noise at the leaf edges and because the leaf widths were much smaller than the leaf lengths. Therefore, the leaf width calculation based on the point cloud data is also challenging during 3D plant phenotyping, causing low correlations of leaf width in such studies.

#### 4.3. Advantages evaluation

The disorder in 3D point clouds disables the direct application of image classification and segmentation frameworks on point clouds. Previously, most research on 3D point cloud segmentation of plants employed traditional heuristic algorithms. Zhu et al. (Zhu et al., 2020) recently used skeletal information to construct an automatic segmentation method for maize stem and leaves. Further, Jin et al. (Jin et al., 2019) proposed a Median normalized-vector growth (MNVG) method for semantic segmentation of the stems and leaves of maize shoots. Although these two approaches achieve good segmentation for individual plants, they require parameter adjustments to obtain the best results, and this adjustment needs to be optimized repeatedly using different inputs. In contrast, DeepSeg3DMaize allows the neural network to be well trained and achieves high segmentation accuracy using a high-quality training dataset. The segmentation of newly

acquired maize point clouds using well-trained models is fully automatic and up-scalable, which is particularly important for achieving high-throughput phenotype extraction. Overall, the deep learning-based approach outperforms the heuristic approach in terms of the automation level and data processing throughput. Although the heuristic algorithm yields better segmentation results with careful manual manipulation, the advantages of automated, high-throughput processing based on deep learning methods are more appropriate for plant phenotypic studies and applications in the context of big data.

In a similar deep learning approach, Shi et al. (2019) proposed segmenting multi-view images via a fully convolutional neural network. The point clouds for stem-leaf segmentation can then be segmented using the image segmentation results. However, this approach can only segment maize seedlings containing two leaves. In later stages of maize growth and development, multi-view images of a shoot could cause significant self-obscurcation, constraining the semantic understanding in image-oriented deep learning models. Thus, the semantic classification results in the model output cannot be echoed, and the complete point cloud cannot be synthesized. Jin et al. (2020) proposed a voxel-based CNN (VCNN) to classify and segment the stems and leaves of individual maize plants from terrestrial LiDAR data. The samples in the dataset were obtained using LiDAR and expanded using leaf translation to achieve data augmentation. However, the diversity of the training dataset is not as impressive as DeepSeg3DMaize. Furthermore, the voxel-based approach may cause data loss by altering the original properties of the point cloud data during voxelization. PointNet was one of the pioneer deep neural networks for processing disordered point cloud data. The method uses input from the original point cloud to preserve the maximum spatial characteristics. PointNet++ (Qi et al., 2017) was designed as an improved version with a new local feature extraction mechanism, which improves the inadequate local feature extraction shortcomings of PointNet. PointNet and PointNet++ have been tested in DeepSeg3DMaize, with the latter identified as much slower. However, there was no discernible difference in accuracy.

#### 4.4. Automated point cloud segmentation approaches promote 3D plant phenotyping

Besides developing DeepSeg3DMaize for maize shoot point cloud segmentation, this study also established a complete phenotyping pipeline, from high-throughput 3D data acquisition to phenotype extraction of maize shoots. The entire process includes high-throughput data acquisition, data pre-processing, data annotation, dataset construction, point cloud segmentation by deep learning, and 3D phenotypes extraction. All aspects of the process can be automated, except data acquisition, shoot transplanting, and manual interaction in data annotation. The high-throughput data acquisition by the MVS-Pheno platform combined with the efficient labelling tools of the Label3DMaize software enabled the construction of high-quality 3D point cloud dataset of maize with satisfactory diversity. The constructed dataset is trained directly on the point cloud using PointNet, and the model can make predictions directly using the point cloud data form. This approach omits the cumbersome data form conversion and improves the efficiency of 3D point cloud data parsing. The entire process from data acquisition to final phenotype extraction achieved in this study has improved the automation of 3D phenotyping of maize plants while ensuring the quality of dataset construction and segmentation accuracy. It is expected to provide a reference for 3D phenotyping of other plants, accelerate plant genetic improvement through accurate high-throughput 3D phenotyping, and contribute to the next revolution in crop breeding (Yang et al., 2020).

## 5. Conclusion

This study presents DeepSeg3DMaize, an automatic 3D point cloud segmentation method for maize plants based on high-throughput data

acquisition and deep neural networks. Accurate segmentation was achieved on testing data at different growth stages, different heights, and leaf numbers. The P (precision), R (recall), and F (F1-Score) for stem-leaf segmentation were 0.91, 0.79, and 0.85, respectively; the P, R and F for organ instance segmentation were 0.94, 0.92, and 0.93, respectively. A high correlation in the six extracted phenotypes was observed when resolved based point cloud segmentation and based on the measured values, indicating that the method can be used for 3D phenotyping of maize plants. DeepSeg3DMaize has been integrated into the MVS-Pheno platform for post-processing to improve the accuracy and efficiency of 3D data processing and phenotypes extraction of maize plants.

## CRediT authorship contribution statement

**Yinglun Li:** Conceptualization, Investigation, Methodology, Visualization, Writing – original draft. **Weiliang Wen:** Funding acquisition, Methodology, Writing – original draft, Writing – review & editing. **Teng Miao:** Formal analysis, Software. **Sheng Wu:** Data curation, Software. **Zetao Yu:** Resources. **Xiaodong Wang:** Validation. **Xinyu Guo:** Conceptualization, Funding acquisition, Supervision, Writing – review & editing. **Chunjiang Zhao:** Funding acquisition, Supervision.

## Declaration of Competing Interest

The authors declare that they have no known competing financial interests or personal relationships that could have appeared to influence the work reported in this paper.

## Acknowledgments

This work was partially supported by Construction of Collaborative Innovation Center of Beijing Academy of Agricultural and Forestry Sciences (No. KJCX201917), Science and Technology Innovation Special Construction Funded Program of Beijing Academy of Agriculture and Forestry Sciences (No. KJCX20210413), the National Natural Science Foundation of China (No. 31871519, No. 32071891), Reform and Development Project of Beijing Academy of agricultural and Forestry Sciences, China Agriculture Research System of MOF and MARA.

## References

- Abendroth, L. E. R., Boyer, M., Marlay, S., 2011. Crecimiento y desarrollo del maíz (Corn Growth and Development Spanish version).
- Barker, J., Zhang, N., Sharon, J., Steeves, R., Wang, X.u., Wei, Y., Poland, J., 2016. Development of a field-based high-throughput mobile phenotyping platform. Computers and Electronics in Agriculture 122, 74–85. <https://doi.org/10.1016/j.compag.2016.01.017>.
- Bernotas, G., Scorza, L., Hansen, M., Hales, I., Halliday, K., Smith, L., McCormick, A., 2019. A photometric stereo-based 3D imaging system using computer vision and deep learning for tracking plant growth. Gigascience 8 (5), 15. <https://doi.org/10.1093/gigascience/giz056>.
- Zhu, C., Miao, T., Xu, T., Yang, T., Li, N., 2020. Stem-leaf segmentation and phenotypic trait extraction of maize shoots from three-dimensional point cloud. cs.CV. doi:arXiv:2009.03108.
- Charles, R.Q., Su, H., Kaichun, M., Guibas, L.J., 2017a. PointNet: Deep Learning on Point Sets for 3D Classification and Segmentation. Paper presented at the 2017 IEEE Conference on Computer Vision and Pattern Recognition (CVPR).
- Chawade, A., van Ham, J., Blomquist, H., Bagge, O., Alexandersson, E., Ortiz, R., 2019. High-Throughput Field-Phenotyping Tools for Plant Breeding and Precision Agriculture. Agronomy-Basel 9 (5), 18. <https://doi.org/10.3390/agronomy9050258>.
- Das Choudhury, S., Maturu, S., Samal, A., Stoerger, V., Awada, T., 2020. Leveraging Image Analysis to Compute 3D Plant Phenotypes Based on Voxel-Grid Plant Reconstruction. Front Plant Sci 11, 521431. <https://doi.org/10.3389/fpls.2020.521431>.
- Dhondt, S., Wuyts, N., Inze, D., 2013. Cell to whole-plant phenotyping: the best is yet to come. Trends in Plant Science 18 (8), 433–444. <https://doi.org/10.1016/j.tplants.2013.04.008>.
- Fasoula, D., Ioannides, I.M., Omirou, M., 2020. Phenotyping and Plant Breeding: Overcoming the Barriers. Frontiers in Plant Science 10. <https://doi.org/10.3389/fpls.2019.01713>.

- Ghahremani, M., Williams, K., Corke, F.M.K., Tiddeman, B., Liu, Y., Doonan, J.H., 2021. Deep Segmentation of Point Clouds of Wheat. 12 (429) <https://doi.org/10.3389/fpls.2021.608732>.
- Ghanem, M.E., Marrou, H., Sinclair, T.R., 2015. Physiological phenotyping of plants for crop improvement. Trends in Plant Science 20 (3), 139–144. <https://doi.org/10.1016/j.tplants.2014.11.006>.
- Goutte, C., Gaussier, E., 2005. A probabilistic interpretation of precision, recall and F-score, with implication for evaluation. In D. E. Losada & J. M. FernandezLuna (Eds.), Advances in Information Retrieval (Vol. 3408, pp. 345–359).
- Charles, R., Yi, L., Su, H., Guibas, L., 2017. PointNet++: Deep Hierarchical Feature Learning on Point Sets in a Metric Space. cs.CV. doi:arXiv:1706.02413v1.
- Guo, Q., Wu, F., Pang, S., Zhao, X., Chen, L., Liu, J., Xue, B., Xu, G., Li, L.e., Jing, H., Chu, C., 2018. Crop 3D-a LiDAR based platform for 3D high-throughput crop phenotyping. Science China-Life Sciences 61 (3), 328–339. <https://doi.org/10.1007/s11427-017-9056-0>.
- Hu, C., Li, P., Pan, Z., 2018. Phenotyping of poplar seedling leaves based on a 3D visualization method. International Journal of Agricultural and Biological Engineering 11 (6), 145–151. <https://doi.org/10.25165/ijabe.20181106.4110>.
- Dutagaci, H., Rasti, P., Galopin, G., Rousseau, D., 2020. ROSE-X: an annotated data set for evaluation of 3D plant organ segmentation methods. Plant Methods 16, 28.
- Jiang, Y., Li, C., Takeda, F., Kramer, E.A., Ashrafi, H., Hunter, J., 2019. 3D point cloud data to quantitatively characterize size and shape of shrub crops. Hortic Res 6, 43. <https://doi.org/10.1038/s41438-019-0123-9>.
- Jin, S., Su, Y., Gao, S., Wu, F., Hu, T., Liu, J., Li, W., Wang, D., Chen, S., Jiang, Y., Pang, S., Guo, Q., 2018. Deep Learning: Individual Maize Segmentation From Terrestrial Lidar Data Using Faster R-CNN and Regional Growth Algorithms. Front Plant Sci 9, <https://doi.org/10.3389/fpls.2018.00866>.
- Jin, S., Su, Y., Gao, S., Wu, F., Ma, Q., Xu, K., Ma, Q., Hu, T., Liu, J., Pang, S., Guan, H., Zhang, J., Guo, Q., 2020. Separating the Structural Components of Maize for Field Phenotyping Using Terrestrial LiDAR Data and Deep Convolutional Neural Networks. IEEE Transactions on Geoscience and Remote Sensing 58 (4), 2644–2658.
- Jin, S., Su, Y., Wu, F., Pang, S., Gao, S., Hu, T., Liu, J., Guo, Q., 2019. Stem-Leaf Segmentation and Phenotypic Trait Extraction of Individual Maize Using Terrestrial LiDAR Data. IEEE Transactions on Geoscience and Remote Sensing 57 (3), 1336–1346.
- Jin, S., Sun, X., Wu, F., Su, Y., Li, Y., Song, S., Xu, K., Ma, Q., Baret, F., Jiang, D., Ding, Y., Guo, Q., 2021. Lidar sheds new light on plant phenomics for plant breeding and management: Recent advances and future prospects. ISPRS Journal of Photogrammetry and Remote Sensing 171, 202–223. <https://doi.org/10.1016/j.isprsjprs.2020.11.006>.
- Kurobe, A., Sekikawa, Y., Ishikawa, K., Saito, H., 2020. CorsNet: 3D Point Cloud Registration by Deep Neural Network. Ieee Robotics and Automation Letters 5 (3), 3960–3966.
- Lee, S.-H., Kim, H.-U., Kim, C.-S., 2019. ELF-Nets: Deep Learning on Point Clouds Using Extended Laplacian Filter. Ieee Access 7, 156569–156581.
- Li, J., Tang, L., 2017. Developing a low-cost 3D plant morphological traits characterization system. Computers and Electronics in Agriculture 143, 1–13. <https://doi.org/10.1016/j.compag.2017.09.025>.
- Li, Z., Guo, R., Li, M., Chen, Y., Li, G., 2020. A review of computer vision technologies for plant phenotyping. Computers and Electronics in Agriculture 176, 21. <https://doi.org/10.1016/j.compag.2020.105672>.
- Lin, Y., 2015. LiDAR: An important tool for next-generation phenotyping technology of high potential for plant phenomics? Computers and Electronics in Agriculture 119, 61–73. <https://doi.org/10.1016/j.compag.2015.10.011>.
- Liu, W., Sun, J., Li, W., Hu, T., Wang, P., 2019. Deep Learning on Point Clouds and Its Application: A Survey. Sensors 19 (19), 4188. <https://doi.org/10.3390/s19194188>.
- Madec, S., Baret, F., de Solan, B., Thomas, S., Dutartre, D., Jezequel, S., Hemmerlé, M., Colombeau, G., Comar, A., 2017. High-Throughput Phenotyping of Plant Height: Comparing Unmanned Aerial Vehicles and Ground LiDAR Estimates. Frontiers in Plant Science 8. <https://doi.org/10.3389/fpls.2017.02002>.
- Miao, T., Wen, W., Li, Y., Wu, S., Zhu, C., Guo, X., 2021. Label3DMaize: toolkit for 3D point cloud data annotation of maize shoots. GigaScience 10 (5), 1–15.
- Mochida, K., Koda, S., Inoue, K., Hirayama, T., Tanaka, S., Nishii, R., Melgani, F., 2019. Computer vision-based phenotyping for improvement of plant productivity: a machine learning perspective. Gigascience 8 (1). <https://doi.org/10.1093/gigascience/giy153>.
- Morel, J., Bac, A., Kanai, T., 2020. Segmentation of unbalanced and in-homogeneous point clouds and its application to 3D scanned trees. Visual Computer 36 (10–12), 2419–2431. <https://doi.org/10.1007/s00371-020-01966-7>.
- Ninomiya, S., Baret, F., Cheng, Z.-M., 2019. Plant Phenomics: Emerging Transdisciplinary Science. Plant Phenomics 2019, 1–3. <https://doi.org/10.34133/2019/2765120>.
- Panjwani, K., Dinh, A., Wahid, K., 2019. LiDARPheno - A Low-Cost LiDAR-Based 3D Scanning System for Leaf Morphological Trait Extraction. Frontiers in Plant Science 10, 17. <https://doi.org/10.3389/fpls.2019.00147>.
- Paulus, S., 2019. Measuring crops in 3D: using geometry for plant phenotyping. Plant Methods 15 (1). <https://doi.org/10.1186/s13007-019-0490-0>.
- Paulus, S., Dupuis, J., Mahlein, A.-K., Kuhlmann, H., 2013. Surface feature based classification of plant organs from 3D laserscanned point clouds for plant phenotyping. Bmc Bioinformatics 14 (1). <https://doi.org/10.1186/1471-2105-14-238>.
- Paulus, S., Dupuis, J., Riedel, S., Kuhlmann, H., 2014. Automated Analysis of Barley Organs Using 3D Laser Scanning: An Approach for High Throughput Phenotyping. Sensors. 14 (7), 12670–12686.
- Perez-Gonzalez, J., Luna-Madrigal, F., Pina-Ramirez, O., 2019. Deep Learning Point Cloud Registration based on Distance Features. IEEE Latin America Transactions 17 (12), 2053–2060.
- Pieruschka, R., Schurr, U., 2019. Plant Phenotyping: Past, Present, and Future. Plant Phenomics 2019, 1–6. <https://doi.org/10.34133/2019/7507131>.
- Qi CR, Yi L, Su H, Guibas LJ, editors. PointNet plus plus : Deep Hierarchical Feature Learning on Point Sets in a Metric Space. 31st Annual Conference on Neural Information Processing Systems (NIPS); 2017 Dec 04–09; Long Beach, CA2017.
- Qi, C., Liu, W., Wu, C., Su, H., Guibas, L., 2018. Frustum PointNets for 3D Object Detection from RGB-D Data. Paper presented at the 2018 IEEE/CVF Conference on Computer Vision and Pattern Recognition.
- Qin, H., Zhang, S., Liu, Q., Chen, L.i., Chen, B., 2020. PointSkelCNN: Deep Learning-Based 3D Human Skeleton Extraction from Point Clouds. Computer Graphics Forum 39 (7), 363–374. <https://doi.org/10.1111/cgf.14151>.
- Qiu, Q., Sun, N.a., Bai, H.e., Wang, N., Fan, Z., Wang, Y., Meng, Z., Li, B., Cong, Y., 2019. Field-Based High-Throughput Phenotyping for Maize Plant Using 3D LiDAR Point Cloud Generated With a “Phenomobile”. Frontiers in Plant Science 10. <https://doi.org/10.3389/fpls.2019.00554>.
- Qiu, R., Wei, S., Zhang, M., Li, H., Sun, H., Liu, G., Li, M., 2018. Sensors for measuring plant phenotyping: A review. International Journal of Agricultural and Biological Engineering 11 (2), 1–17. <https://doi.org/10.25165/ijabe.20181102.2696>.
- Shi, W., Zedde, R., Jiang, H., Kootstra, G., 2019. Plant-part segmentation using deep learning and multi-view vision. Biosystems Engineering 187, 81–95. <https://doi.org/10.1016/j.biosystemseng.2019.08.014>.
- Singh, A., Ganapathysubramanian, B., Singh, A.K., Sarkar, S., 2016. Machine Learning for High-Throughput Stress Phenotyping in Plants. Trends Plant Sci. 21 (2), 110–124.
- Song, Y., Gao, L., Li, X., Shen, W., 2020. A Novel Point Cloud Encoding Method Based on Local Information for 3D Classification and Segmentation. Sensors 20 (9), 2501. <https://doi.org/10.3390/s20092501>.
- Tardieu, F., Cabrera-Bosquet, L., Pridmore, T., Bennett, M., 2017. Plant Phenomics, From Sensors to Knowledge. Current Biology 27 (15), R770–R783. <https://doi.org/10.1016/j.cub.2017.05.055>.
- Turgut, K., Dutagaci, H., Galopin, G., Rousseau, D., 2020. Segmentation of structural parts of rosebush plants with 3d point-based deep learning methods. ArXiv: 2012.11489v1 [cs.CV], 2020.
- Ubbens, J., Stavness, I., 2018. Deep Plant Phenomics: A Deep Learning Platform for Complex Plant Phenotyping Tasks (vol 8, 1190, 2017). Frontiers in Plant Science 8, 1. <https://doi.org/10.3389/fpls.2017.02245>.
- Walter, J., Edwards, J., McDonald, G., Kuchel, H., 2019. Estimating Biomass and Canopy Height With LiDAR for Field Crop Breeding. Frontiers in Plant Science 10, 16. <https://doi.org/10.3389/fpls.2019.01145>.
- Wang, Y., Wen, W., Wu, S., Wang, C., Yu, Z., Guo, X., Zhao, C., 2018. Maize Plant Phenotyping: Comparing 3D Laser Scanning, Multi-View Stereo Reconstruction, and 3D Digitizing Estimates. Remote Sensing 11 (1), 63. <https://doi.org/10.3390/rs1110063>.
- Wu, J., Cawse-Nicholson, K., Aardt, J., 2013. 3D Tree Reconstruction from Simulated Small Footprint Waveform Lidar. Photogrammetric Engineering and Remote Sensing 79 (12), 1147–1157. <https://doi.org/10.14358/pers.79.12.1147>.
- Wu, S., Wen, W., Wang, Y., Fan, J., Wang, C., Gou, W., Guo, X., 2020. MVS-Pheno: A Portable and Low-Cost Phenotyping Platform for Maize Shoots Using Multiview Stereo 3D Reconstruction. Plant Phenomics 2020, 1–17. <https://doi.org/10.34133/2020/1848437>.
- Wu, S., Wen, W., Xiao, B., Guo, X., Du, J., Wang, C., Wang, Y., 2019. An Accurate Skeleton Extraction Approach From 3D Point Clouds of Maize Plants. Frontiers in Plant Science 10, 14. <https://doi.org/10.3389/fpls.2019.00248>.
- Yang, W., Feng, H., Zhang, X., Zhang, J., Doohan, J.H., Batchelor, W.D., Xiong, L., Yan, J., 2020. Crop Phenomics and High-Throughput Phenotyping: Past Decades, Current Challenges, and Future Perspectives. Mol Plant 13 (2), 187–214. <https://doi.org/10.1016/j.molp.2020.01.008>.
- Yang, X., Gao, S., Xu, S., Zhang, Z., Prasanna, B.M., Li, L., Li, J., Yan, J., 2010. Characterization of a global germplasm collection and its potential utilization for analysis of complex quantitative traits in maize. Molecular Breeding 28 (4), 511–526. <https://doi.org/10.1007/s11032-010-9500-7>.
- Yang, X., Strahler, A., Schaaf, C., Jupp, D., Yao, T., Zhao, F., Ni-Meister, W., 2013. Three-dimensional forest reconstruction and structural parameter retrievals using a terrestrial full-waveform lidar instrument (Echidn (R)). Remote Sensing of Environment 135, 36–51. <https://doi.org/10.1016/j.rse.2013.03.020>.
- Yizong, C., 1995. Mean shift, mode seeking, and clustering. IEEE Transactions on Pattern Analysis and Machine Intelligence. 17 (8), 790–799.
- Yin, K., Huang, H., Cohen-Or, D., Zhang, H., 2018. P2P-NET: bidirectional point displacement net for shape transform. ACM Trans. Graph. 37 (4), 1–13.
- Zhao, B., Hua, X., Yu, K., Tao, W., He, X., Feng, S., Tian, P., 2020. Evaluation of Convolution Operation Based on the Interpretation of Deep Learning on 3-D Point Cloud. Ieee Journal of Selected Topics in Applied Earth Observations and Remote Sensing 13, 5088–5101.
- Zhao, C., 2019. Big Data of Plant Phenomics and Its Research Progress. Journal of Agricultural Big Data 1 (2), 5–18. <https://doi.org/10.19788/j.issn.2096-6369.190201>.
- Zhao, C., Zhang, Y., Du, J., Guo, X., Wen, W., Gu, S., Fan, J., 2019. Crop Phenomics: Current Status and Perspectives. Front Plant Sci 10, 714. <https://doi.org/10.3389/fpls.2019.00714>.

- Zhong, Y., 2010. Intrinsic shape signatures: A shape descriptor for 3D object recognition. Paper presented at the IEEE International Conference on Computer Vision Workshops.
- Ziamtsov, I., Navlakha, S., 2019. Machine Learning Approaches to Improve Three Basic Plant Phenotyping Tasks Using Three-Dimensional Point Clouds. *Plant Physiol* 181 (4), 1425–1440. <https://doi.org/10.1104/pp.19.00524>.
- Ziamtsov, I., Navlakha, S., 2020. Plant 3D (P3D): a plant phenotyping toolkit for 3D point clouds. *Bioinformatics* 36 (12), 3949–3950. <https://doi.org/10.1093/bioinformatics/btaa220>.